Journal of Applied Physics

Probing the impact of carbon quantum dots on partially unwound helical mode in ferroelectric liquid crystals

Cite as: J. Appl. Phys. **125**, 125108 (2019); https://doi.org/10.1063/1.5082903
Submitted: 26 November 2018 . Accepted: 08 March 2019 . Published Online: 27 March 2019

Lokesh K. Gangwar, Aditya Kumar, Gautam Singh, Amit Choudhary, Rajesh, Surinder P. Singh, and Ashok M. Biradar

Journal of Applied Physics ARTICLE scitation.org/journal/jap

Probing the impact of carbon quantum dots on partially unwound helical mode in ferroelectric liquid crystals

Cite as: J. Appl. Phys. **125**, 125108 (2019); doi: 10.1063/1.5082903
Submitted: 26 November 2018 · Accepted: 8 March 2019 ·
Published Online: 27 March 2019

Lokesh K. Gangwar,[1,2] Aditya Kumar,[3] Gautam Singh,[3,a)] Amit Choudhary,[4,a)] Rajesh,[2] Surinder P. Singh,[2] and Ashok M. Biradar[2]

AFFILIATIONS

[1]Academy of Scientific and Innovative Research (AcSIR), CSIR-National Physical Laboratory (CSIR-NPL) Campus, New Delhi 110012, India
[2]CSIR-National Physical Laboratory, Dr. K. S. Krishnan Marg, New Delhi 110012, India
[3]Department of Applied Physics, Amity Institute of Applied Sciences, Amity University, Noida, Uttar Pradesh 201313, India
[4]Physics Department, Deshbandhu College, University of Delhi, Kalkaji, New Delhi 110019, India

[a)]**Authors to whom correspondence should be addressed:** amitnpl2005@gmail.com and gsingh6@amity.edu

ABSTRACT

We report the modulation in dielectric properties of a ferroelectric liquid crystal (FLC) by using carbon quantum dots (CQDs) of size ~4–5 nm. The appearance of a low frequency dielectric relaxation mode in the FLC, called the partially unwound helical mode (*p*-UHM), is controlled by CQDs with a FLC material in two different ways. Firstly, CQDs are dispersed into the bulk of the FLC before filling into a sample cell, and secondly, they are deposited onto the surface of a substrate. In both cases, the *p*-UHM has been found suppressed due to the modulation of a helicoidal structure at the interface of the FLC and the surface of the substrate of the sample cell. It has also been confirmed that CQDs at the interface of the FLC and the surface of the substrate have not affected the intrinsic properties of the FLC material. On the other hand, CQDs in the bulk of the FLC have shown remarkable variations in the fundamental properties of the FLC material. The suppression of the dielectric mode is confirmed by high-resolution dielectric spectroscopy, optical textures, and contact angle measurements. The concept of appearance and disappearance of the *p*-UHM process leads to the understanding of FLC systems in confined geometries for various display and non-display applications.

INTRODUCTION

It is a well-known fact that the surface anchoring of a substrate having a conducting and transparent coating with ferroelectric liquid crystals (FLCs) plays a crucial role in the behaviour of a helicoidal structure at bounding surfaces and in the bulk of FLCs. The substrate surface treatments have modulated the molecular dynamics in the sample cell and resulted in the various display applications. The memory effect is one of the vital outcomes of the substrate surface anchoring of FLC molecules, wherein the sample cell thickness should be less than the helical pitch value of the FLC director.[1] This type of sample is known as a surface stabilized FLC (SSFLC) cell. However, it has been observed that in some of the FLC materials, the cell thickness is no longer a critical parameter for the observance of the memory effect in FLCs. This is due to the fact that the memory effect is also observed in the sample cells of the FLCs where the thickness of the sample is more than the helical pitch value of the those FLCs.[1–4] The various surface treatments over the substrate are efficiently used to control the defects in SSFLC samples and show their significance in display devices.[5,6]

Dielectric relaxation processes are the key tool to study the FLC material under various configurations of substrates and temperatures. The thick polymer alignment layer at the interface of FLCs and substrate surfaces has been found to accumulate electrostatic charges caused by strong rubbing on the polymer layer. Such a thick polymer alignment layer is found responsible for a dielectric relaxation phenomenon at the sub-hertz frequency range.[7,8] In an SSFLC

system, the surface alignment layer dominates the material behavior.[9] Meyer in 1977 proposed the concept of helical unwinding by the application of an external electric field.[10] The helical unwinding process is also achieved by shear flow[11] and the effect of surface anchoring of the substrate.[12–14] The two dielectric relaxation processes corresponding to winding and unwinding have been observed in the FLC material, resulting in two different time scales. The dielectric relaxation process of helical winding is slower than the unwinding due to its dependence on material parameters. For instance, the unwinding process of a helical structure is dependent on the applied electric field (amplitude and frequency), whereas the winding process is natural and takes a longer time and hence is slower than the unwinding.[15]

It is well known that in smectic layers, the molecular director constitutes the helical structure which is represented by the smectic pseudo-cone. This cone is constituted by the tilt and phase angles of molecules in the layer of the chiral smectic C (SmC*) phase of liquid crystals. The trajectory of the molecular director orientation from one layer to another in SmC* is through the surface of this smectic cone. The complete cycle of the molecular director over the cone corresponds to the one complete helical pitch. In dielectric spectroscopy, the dielectric relaxation process corresponding to the phase (azimuthal angle) fluctuations is called the "phason mode," which is observed in the SmC* phase. This phason mode in the SmC* phase is also known as the Goldstone mode (GM) due to the spontaneous symmetry breaking concept across the phase transition from the chiral smectic A (SmA*) to the SmC* phase. This mode is proposed by J. Goldstone[16] in the theory of superconductors in 1961 with the spontaneous symmetry breaking concept as proposed by Nambu in 1960.[17] Furthermore, this concept of spontaneous symmetry breaking is used to describe the transition of FLC from the SmC* to the SmA* phase. In FLC materials, the continuous cylindrical symmetry is reduced to C_2 symmetry due to a spontaneous breaking of the mirror and centro-symmetry on cooling the material from the SmA* to the SmC* phase.[18] Due to this reduction in symmetry, the relaxation process in the SmC* phase is named after J. Goldstone as the Goldstone mode. The Goldstone mode is almost temperature independent throughout the SmC* phase, whereas the soft mode relaxation process is found to be strongly temperature dependent near the transition temperature (T_c) in both the SmC* and the SmA* phases. The tilt fluctuations (the amplitude of the tilt angle) give rise to the soft mode dielectric relaxation process near T_c in the SmC* and SmA* phases. These processes contribute to the dielectric strength at low frequencies of FLC which is reflected in the dielectric spectroscopy. It has been theoretically proposed that the dielectric strength of FLC at low frequency is the contribution of two dielectric processes; i.e., one is the fluctuation in the phase of the tilt angle and the other is the fluctuation in the unwinding of a complete helicoidal structure.[19] The low frequency dielectric relaxation process along with GM is observed in the ferrielectric liquid crystal, which is called ferrielectric GM.[20] The ferrielectric phase is the intermediate phase between the antiferroelectric and the ferroelectric phases of liquid crystals having the same symmetry as SmC* and a smaller helicoidal pitch than SmC*.[21] In FLC systems, such a lower frequency process other than GM has been observed experimentally in the highly anchored sample cell of appropriate thickness (~8–20 μm).[12–14] It has been interpreted as the partial unwinding of the helicoidal structure at the interface of the solid substrate surface and FLC material, leading to a separate dielectric relaxation process at a lower frequency than GM frequency. Interestingly, this contributes significantly to the dielectric strength of the FLC material at the low frequency region in the SmC* phase.[12]

Recently, it has been found that the doping of carbon nanomaterials (quantum dots, rods, tubes, etc.) into LCs (nematic, chiral nematic, and FLC) resulted in significant modifications in the physical properties of LCs, which eventually impacted the current LC technology.[22–28] More importantly, carbon quantum dots (CQDs) are found to be more suitable as a dopant into LCs due to their size (~2–10 nm), shape (quasi-spherical), and tunable electronic, chemical, and optical properties.[29–36] Consequently, CQDs have been doped into various FLC systems in order to tune their optical, dielectric, and electro-optical properties.[37–40] It is worth pointing out here that despite various useful results of CQDs-LC nanocomposites, the mechanism involved in the interaction between CQDs and LCs (especially FLCs) is rather unclear. A study of the effect of CQDs on the surface anchoring energy between solid substrates and FLC molecules might help in the understanding of the mechanism of modulation in helicoidal structures. Since CQDs control the helicoidal structures of FLC systems which could affect the dielectric, optical, and electro-optical properties of FLCs, a detailed dielectric spectroscopy, along with contact angle measurements and optical studies, would be helpful for understanding the mechanism. To the best of our knowledge, no such studies have been reported on CQDs-FLCs' nanocomposites and hence it would be worth doing detailed investigations on these systems.

In this paper, we mainly focus on the effect of CQDs on the dielectric properties of FLC due to the suppression of helical unwinding at the interface of FLC and the solid substrate of the sample cell. The implementation of CQDs with FLC has been done in two different ways: (i) dispersing CQDs into the bulk of the FLC matrix and (ii) depositing CQDs on highly anchored substrate surfaces (strongly rubbed nylon 6/6 coated surfaces). By using high resolution frequency domain dielectric spectroscopy, we study the effect of CQDs on the partially unwound helical mode (p-UHM), which usually appears along with the GM in FLCs by employing the highly anchored surfaces in a sample cell.[12] Moreover, high resolution optical textures and contact angle measurements are also performed in order to understand the interface interaction between FLC molecules and CQDs' deposited surfaces. The appearance of the p-UHM could be realized in a large FLC family. The enhancement in the dielectric properties at a lower frequency due to the appearance of the p-UHM is made tunable by CQDs. The switching under the p-UHM gives rise to the possibility of switching the device without affecting the bulk molecular arrangement at lower frequencies and lower amplitudes of applied fields than those under the conventional molecular switching.[12]

EXPERIMENTAL

Indium tin oxide (ITO) coated glass plates were used as the substrates for preparing liquid crystal sample cells. A desired pattern of a 4 mm × 4 mm area of ITO was prepared on the glass

plates using the photolithography technique. The ITO patterned, highly anchored glass substrates were prepared by coating a thick polymer of nylon 6/6 and rubbed strongly to align the FLC molecules. The nylon coated and strongly rubbed ITO patterned glass substrates were then assembled using 8 μm thick Mylar spacers. The FLC material KCFLC 10S (Kingston Chemicals, UK) was filled into the sample cell by heating the material at its isotropic phase (~120 °C). The phase sequence of investigated FLC material is

$$\text{Crystalline} \overset{?}{\longleftrightarrow} \text{SmC}^{\star} \overset{64.5^{\circ}C}{\longleftrightarrow} \text{SmA}^{\star} \overset{99.5^{\circ}C}{\longleftrightarrow} \text{Nematic} \overset{112^{\circ}C}{\longleftrightarrow} \text{Isotropic}.$$

The CQDs were synthesized by a hydrothermal treatment of gelatin in the presence of pure water[22] and characterized using the transmission electron microscope (TEM), FEI Technai G2 F20, operated at 200 kV. CQDs were originally dispersed in water. However, the addition and evaporation of water from the FLC matrix is very difficult; therefore, the solvent of CQDs was changed from water to ethanol, wherein ethanol can be evaporated easily from the FLC matrix. The three sample cells of the different configurations were prepared. **S1** is the sample with a strong rubbing (i.e., a strong anchoring) of a nylon 6/6 coated substrate; **S2** is the sample with 5 wt. % CQDs dispersed into the FLC material; and **S3** is the sample with CQDs deposited on the strongly rubbed nylon 6/6 alignment layer. The CQDs were dispersed into the bulk of the FLC as sample **S2**, and an ethanol solvent was evaporated at 120 °C in the isotropic phase of the FLC material to ensure the complete evaporation of the solvent and proper dispersion of CQDs. For sample **S3**, the CQDs were deposited uniformly over the strongly rubbed nylon surfaces using the drop cast method and the solvent (ethanol) was evaporated at ~70 °C.

The alignment of FLC molecules in all the three types of sample cells (**S1**, **S2**, and **S3**) was examined under the high-resolution cross-polarised optical microscope (Carl Zeiss, Axioskop 40A, Germany). Dielectric spectroscopy was carried out in these three sample cells by an impedance analyser (Wayne Kerr 6540A, UK) at a frequency range of 20 Hz to 1 MHz and the probing ac field was varied from 30 mV to 1 V. The surface energy of the substrates was measured using contact angle measurements (Drop Shape Analysis System, model DSA10MK2 from Krüss GmbH, Germany). The temperature dependent studies were carried out by controlling the temperature of the sample cell holder using a temperature controller with accuracy ±0.1 °C (Julabo-25 HE, Germany).

RESULTS AND DISCUSSIONS

The CQDs dispersed in water are characterized by the transmission electron microscope (TEM), as shown in Fig. 1. The size of the CQDs is observed to be ~4–5 nm. Since the sizes of the CQDs and the FLC molecules are comparable, there is not much distortion expected in the alignment of the FLC molecular director, unlike larger size micro/nanoparticles. This effect can be realized in the cross-polarized optical micrographs.

All the three samples (**S1**, **S2**, and **S3**) are characterized using dielectric spectroscopy to observe the low frequency process along with GM. Figure 2 shows the dielectric permittivity and loss tangent (tanδ) as a function of frequency at different probing ac

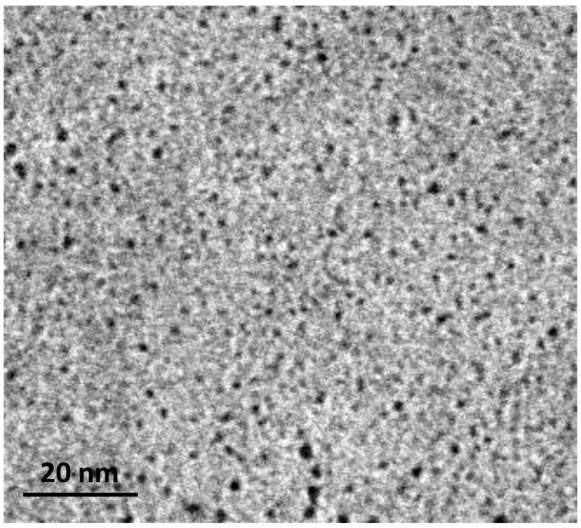

FIG. 1. Transmission electron microscopic image of carbon quantum dots (CQDs). The size of the CQDs is ~4 to 5 nm.

voltages at room temperature. As seen in Fig. 2(a), at low probing voltages, the dielectric permittivity of **S1** is low, and as the probing voltage increases, the permittivity also increases, which becomes maximum at around 300 mV. This increment in permittivity with high probing ac voltages indicates the possibility of the existence of more than one dielectric process. This is clearly reflected in the observation of the low frequency process along with GM in the tan δ vs frequency plot [Fig 2(b)]. One process at the higher frequency is due to the well-known GM and the other process at the lower frequency is due to the *p*-UHM process, which is clearly seen at 300 mV probing ac voltages and described in detail somewhere else.[12–14] The relaxation frequency of the *p*-UHM is found to increase with the increase in applied probing ac voltage, confirming the existence of partial unwinding of a helicoidal structure at the interface of FLC and the substrate surface of the sample cell.[12–14]

To understand and exploit the impact of CQDs on the properties and the existence of the *p*-UHM process in FLC material, the **S2** and **S3** are characterised by high resolution dielectric spectroscopy. In Figs. 2(c) and 2(d), the probing ac voltage dependent dielectric measurements on the **S2** sample are performed for the observation of the *p*-UHM process. The dielectric permittivity is found almost independent of the applied probing ac voltages at room temperature. However, the small increment in the dielectric permittivity at low frequency (i.e., from 55 to 63 at 30 mV to 1 V, respectively) is observed, as shown in Fig. 2(c). In tanδ graph, only one dielectric relaxation process (i.e., GM) independent of the amplitude of applied probing ac voltage is observed [Fig. 2(d)]. This has certainly ruled out the presence of any relaxation mode due to the partially unwound helix. It is worth mentioning here that all the parameters are kept constant in all the sample cells (**S1**, **S2**, and **S3**) except the dispersion of CQDs. Therefore, the observation of the disappearance of the *p*-UHM clearly indicates a suppression of the *p*-UHM by CQDs on the dynamics of the FLC molecules at the interface of

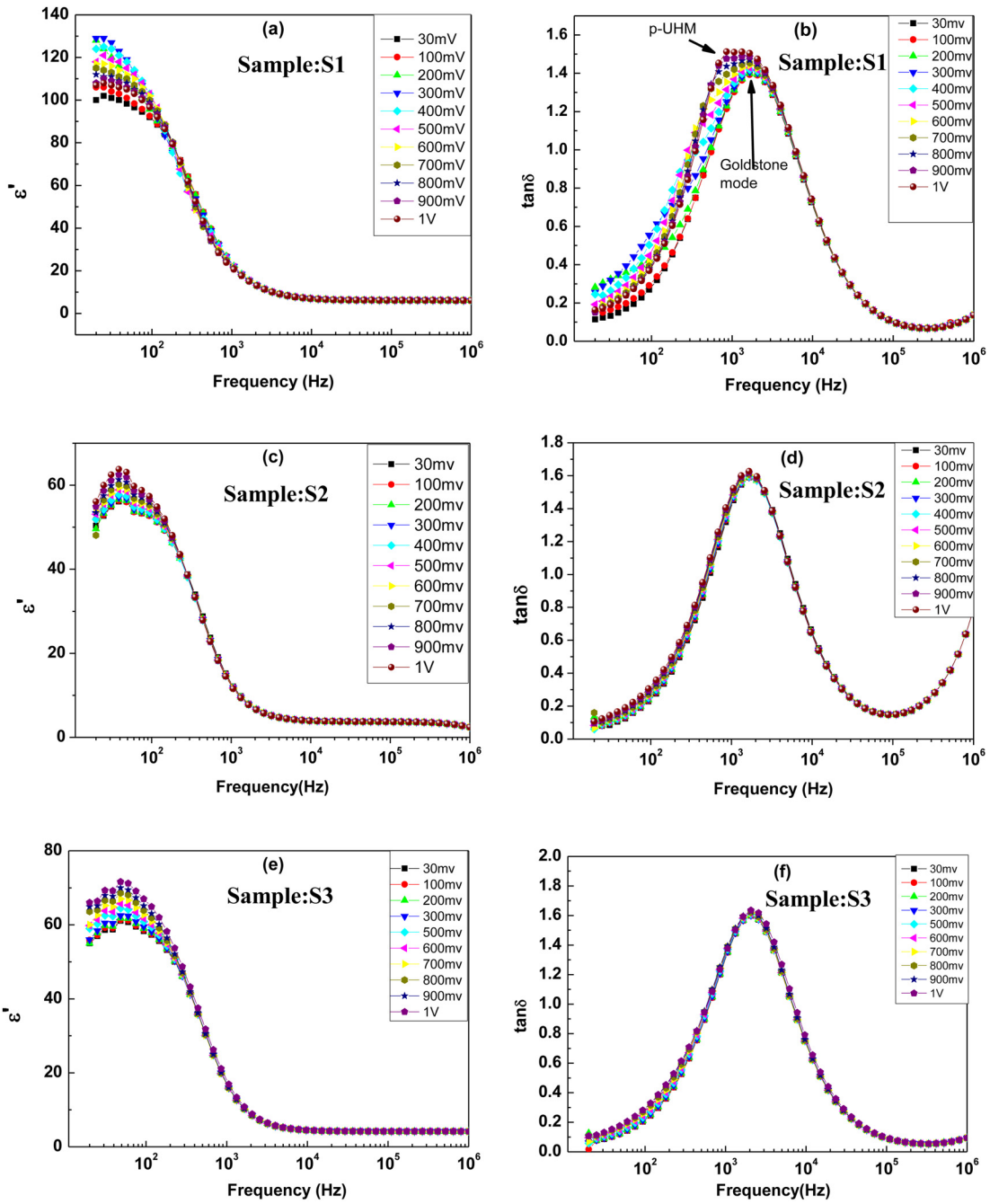

FIG. 2. Dielectric spectra at various amplitudes of probing ac voltages at room temperature of (a) and (b) pure FLC, (c) and (d) CQDs' dispersed FLC nanocomposite, and (e) and (f) CQDs deposited on the surface of the substrate.

FLC and the solid substrate surface of the sample cell. If this consideration of the interfacial impact of CQDs in the bulk of the FLC is true, then the direct deposition of CQDs on the substrate of the sample cell could also affect the dynamics of FLC molecules at the interface of the FLC and the substrate surface of the cell. Therefore, CQDs are deposited on the substrate surface in the **S3** sample. As seen in Figs. 2(e) and 2(f), the dielectric permittivity (ε′) at low frequencies is drastically reduced to about half of the **S1** sample cell.

Such a reduction in dielectric permittivity has also been observed in the case of the **S2** sample cell. The dielectric permittivity has shown a slight increment from 60 at 30 mV to 70 at 900 mV [Fig. 2(e)]. On the other hand, the tanδ graph shows the existence of only the single dielectric relaxation process which is the well-known GM and is found independent on the amplitude of the probing ac voltage [Fig. 2(f)]. This means that the *p*-UHM disappears upon introducing the CQDs into the bulk of FLC and at the interface of the the FLC and the solid substrate surface.

As discussed above, the *p*-UHM is not observed at room temperature in the **S3** sample cell; therefore, the temperature dependent measurements were carried out in the **S1**, **S2**, and **S3** sample

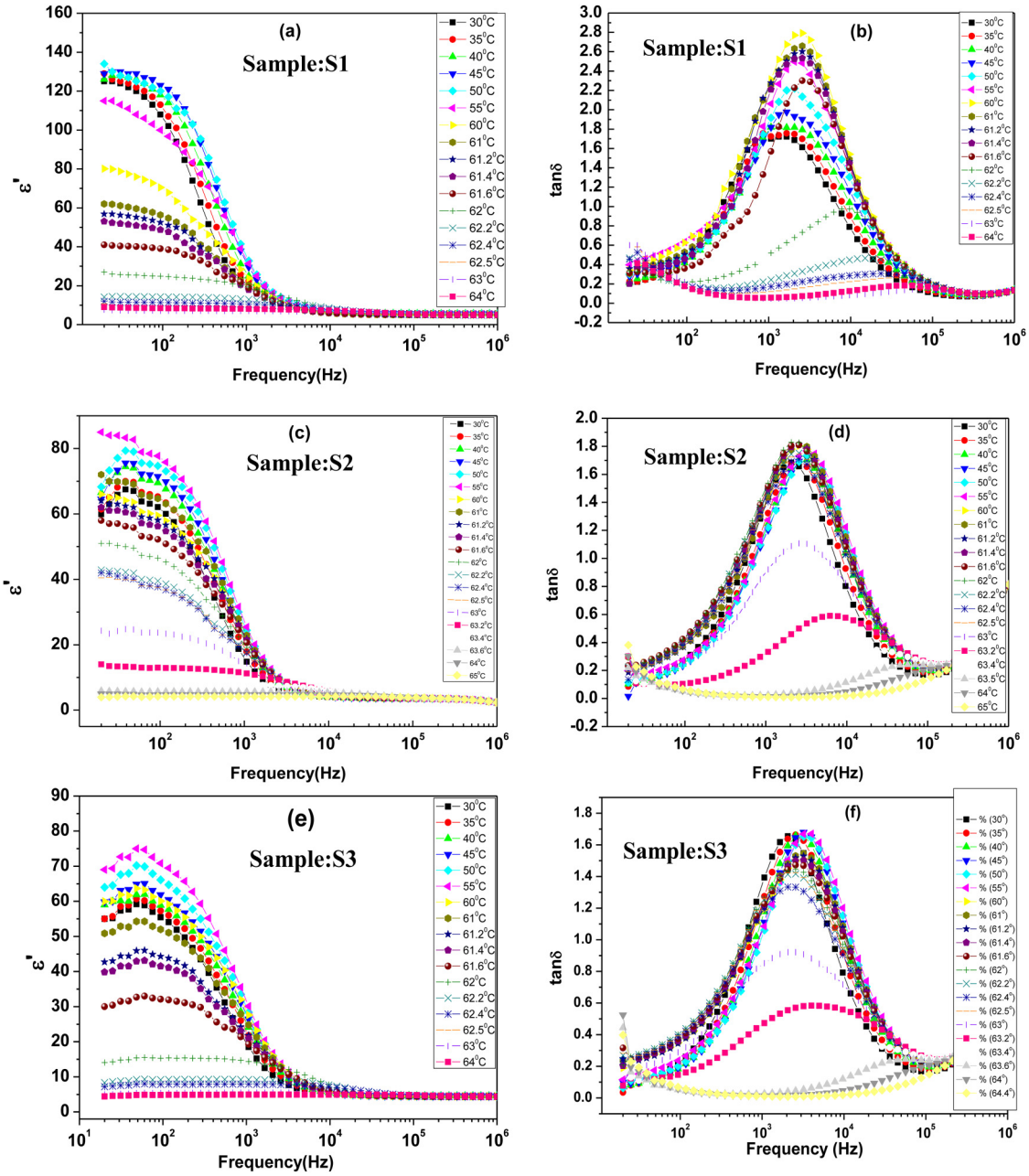

FIG. 3. Dielectric spectra at various temperatures at 1 V amplitude of probing ac voltage of (a) and (b) pure FLC, (c) and (d) CQDs' dispersed FLC nanocomposite, and (e) and (f) CQDs deposited on the surface of the substrate.

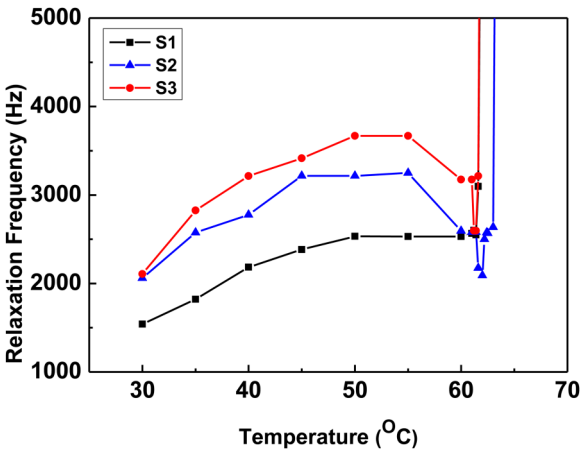

FIG. 4. Dielectric relaxation frequency of GM for all the three FLC systems as a function of temperature at 1 V amplitude of probing ac voltage.

cells [Fig. 3]. Figure 3(a) shows the dielectric permittivity of the **S1** sample cell that shows the transition temperature (T_c) at 62 °C. The dielectric permittivity has shown an increment from 143 to 162 at low frequency up to 55 °C and starts decreasing afterwards. The same behavior of the materials is confirmed by the tanδ curves also, in which the existence of the *p*-UHM is seen clearly [Fig. 3(b)]. Figures 3(c) and 3(d) show the temperature dependent dielectric permittivity of the **S2** sample cell. The dielectric permittivity is lower at room temperature in comparison with the **S1** sample, suggesting the presence of GM only [Fig. 3(c)]. The dielectric strength is found to increase with temperature up to 55 °C, unlike in pure FLC, where it is almost constant till 50 °C and decreases afterwards. The tanδ vs frequency response suggests only a single dielectric relaxation peak of the GM process and does not show any indication of *p*-UHM even at the close vicinity of T_c [Fig. 3(d)]. There is only a soft mode relaxation process which is the characteristic of the SmA* phase after T_c. It is worth pointing out here that T_c of the SmC*-SmA* phase transition is increased by ~1.6 °C in **S2** when compared with **S1**.

Now, the temperature-dependent dielectric studies of the **S3** sample cell have been carried in the SmC* and SmA* phases to unveil the outcome of surface modification on the dielectric properties of the FLC/CQD system. The pure FLC is sandwiched between two CQD deposited surfaces, resulting in the reduced dielectric permittivity as in the case of the **S2** sample cell [Fig. 3(e)]. Here also, the dielectric permittivity is found increasing up to 55 °C and then decreasing up to T_c (62 °C) like in the **S1**. Figure 3(f) shows only the GM process, which remains almost stagnant at the same frequency throughout the whole temperature range. Figure 4 shows the GM dielectric relaxation frequencies as a function of temperature. The incorporation of CQDs with the FLC system has clearly shifted the dielectric relaxation peak process of GM. The surface effect of CQDs (**S3**) has shifted the process towards the higher frequencies largely in comparison with the CQDs dispersed into the bulk of the FLC system (**S2**). The shift in relaxation is interpreted on the basis of the surface bound FLC molecules which are held more tightly at the substrate surface of **S3** in comparison with the bulk molecules up to some extent, causing the shift in the relaxation frequency. However, in the pure FLC sample cell **S1** with strongly anchored surfaces, the helical structure at the interface is partially unwound, which leads to the observation of the *p*-UHM process, whereas in the **S2** and **S3** sample cells, this process is missing due to changes in the features caused by the interference of CQDs with the FLC helicoidal structure.

Another significant observation is the shift in T_c of the **S2** sample. We have seen that the actual transition temperature of pure FLC is found lower than the reported 64.5 °C in the data sheet of the KCFLC 10S material. This is due to the fact that the surface plays a very important role in slightly shifting the properties of FLCs.[41] The sample cells in the present study have been made using strongly anchored surfaces and maintaining the spacing between the substrates of around 8 μm. Therefore, the decrement in T_c of FLC in confined geometry is a natural process restricted by the surfaces of the cell.

In all the above results and discussions of **S1**, **S2**, and **S3**, there are two important comparable points to be noticed: two types of sample cell surfaces (**S1** and **S3**) and two types of FLC configurations (**S1** and **S2**) have been studied for the observation of *p*-UHM. In the two comparable surfaces, **S1** and **S3**, the FLC material is pure FLC (KCFLC 10S) and the impact on the dielectric properties is observed only due to the surface. Whereas in the two comparable FLC systems, the pure (**S1**) and CQDs' dispersed FLC systems (**S2**), the variation in the dielectric properties is due to the dispersion of CQD in FLC, while the surfaces of the substrates remain the same. The optical textures and contact angle measurement studies have been carried out to affirm the impact of these conditions, keeping the rest of the parameters (cell thickness, rubbing strength, temperature, and measurement conditions) same

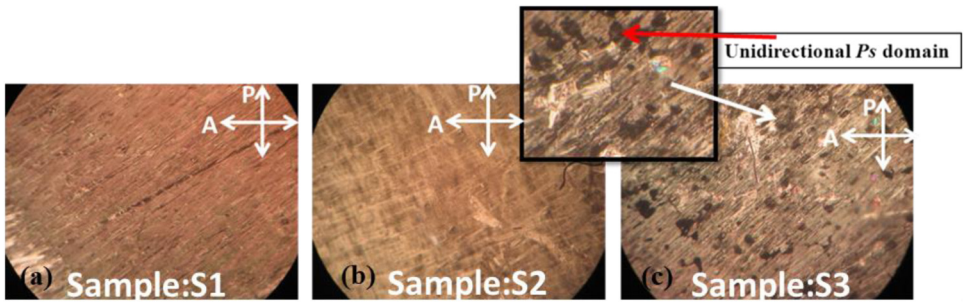

FIG. 5. Optical micrographs of (a) pure FLC, (b) CQDs' dispersed FLC nanocomposite, and (c) CQDs deposited on the surface of the substrate under cross polarizers of the polarizing optical microscope.

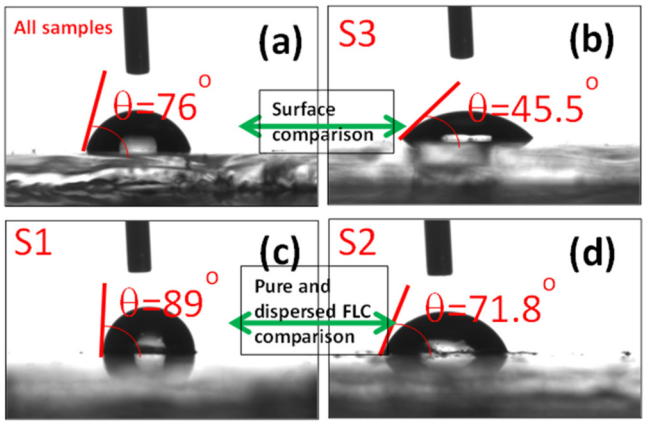

FIG. 6. Contact angle measurements of (a) the strongly rubbed nylon 6/6 surface as used for all the samples, (b) CQDs deposited on the strongly rubbed surface of nylon 6/6 as used in **S3**, (c) pure FLC (KCFLC 10S) spread uniformly on the strongly rubbed surface of nylon 6/6, as used in **S1**, and (d) CQDs' dispersed FLC nanocomposite spread uniformly on the strongly rubbed surface of nylon 6/6 as used in **S2**.

for all the samples. Figures 5(a)–5(c) show the optical textures of all the three samples. The comparison of the optical micrographs reveals the distinction in the molecular alignment due to modifications in the surface adhesion of the substrates (**S3**) and the surface tension of the FLC made by the dispersion of CQDs (**S2**) in comparison with **S1**. The textures of Figs. 5(a) and 5(b) are almost the same except that the texture in Fig. 5(b) is a little bit scattered in comparison with **S1**. This is due to the change in the internal energy of the FLC system which is modified by the interaction between the CQD and the FLC, i.e., the surface tension of FLC. On the other hand, in the optical texture of Fig. 5(c), the localized monostable domains are seen due to the modified surface energy of the substrate by deposited CQDs (**S3**). This confirms that the modification in the optical textures of **S1**, **S2**, and **S3** are due to substrate interaction with FLC, i.e., the anchoring energy of the substrate, but still it is significant to see whether the anchoring energy of the substrate is increased or decreased in all the configurations, which is done by contact angle measurements of the above configurations.

Figure 6 shows the contact angle studies of the configurations in the **S1**, **S2**, and **S3** sample cells in the following ways. The contact angle measurement is performed on a strongly rubbed nylon 6/6 substrate (which is used for all samples), pure FLC on a strongly rubbed nylon 6/6 (**S1**), a thin film of CQDs dispersed FLC (**S2**), and CQDs deposited on the substrate surface (**S3**). Figures 6(a) and 6(b) show the comparison of the two types of surfaces as bare nylon 6/6 and CQDs dispersed on nylon 6/6. Figure 6(a) is the contact angle measurement of the strongly anchored nylon 6/6 substrate surface that develops the contact angle of 76°. On the other hand, the CQDs deposited on the substrate surface as used in **S3** have shown the reduced contact angle of 45.5°. The solid-liquid adhesion energy W_{SL} is estimated by Young's equation:[42] $W_{SL} = \gamma_L(1 + \cos\theta)$, where θ is the contact angle and γ_L is the surface tension of water (71.9 N/m at 25 °C) which is dropped on the substrate surface.[43] The CQDs have offered the increased surface adhesion energy of 122.3 mJ/m^2 at 45.5° to the substrate for FLC in comparison with the bare nylon 6/6 rubbed surface with 89 mJ/m^2 at 76° to the FLC material. The larger the surface adhesion energy, the more will be the anchoring of FLC molecules on the surface and the larger will be the helical unwinding due to which no *p*-UHM process is observed in the dielectric spectra, as shown in Figs. 2(e) and 2(f).

Figures 6(c) and (6d) show the comparison of FLCs in pure form as in **S1** and CQDs dispersed in FLC material as in **S2**. The highly anchored surfaces are prepared for pure FLC as in **S1** and CQDs dispersed FLC as in **S2**. The CQDs dispersed FLC is uniformly spread over the rubbed nylon 6/6 for the contact angle measurement. The FLC materials are uniformly spread over the substrate above the isotropic transition temperature of 120 °C of FLC. The reduced contact angle of CQDs' dispersed FLC nanocomposites points towards an increase in surface tension 94.35 mJ/m^2 in comparison with pure FLC 73.15 mJ/m^2. The increase in the surface tension of CQDs' dispersed FLC nanocomposites is because of the intermolecular interaction of FLC mediated by CQDs. This is also confirmed by the phase transition study in which T_c is found to be increased by ~1.5 °C in the CQDs' dispersed FLC nanocomposite **S2** sample. Here, the increased surface tension of the FLC composites has not allowed the strong FLC molecular interaction with the bare nylon 6/6 interaction and hence the helix is not sufficiently allowed to generate the *p*-UHM process [Figs. 2(c) and 2(d)]. The *p*-UHM is not observed in the dielectric measurements; therefore, its contribution to dielectric permittivity is also not observed and hence the lower value of dielectric permittivity in both the cases of CQDs, **S2** and **S3** samples.

The schematic of the helicoidal structure of FLC at the interface of FLC and strongly rubbed surfaces is illustrated in Fig. 7. The FLC material and the rubbed surfaces are modified by CQDs,

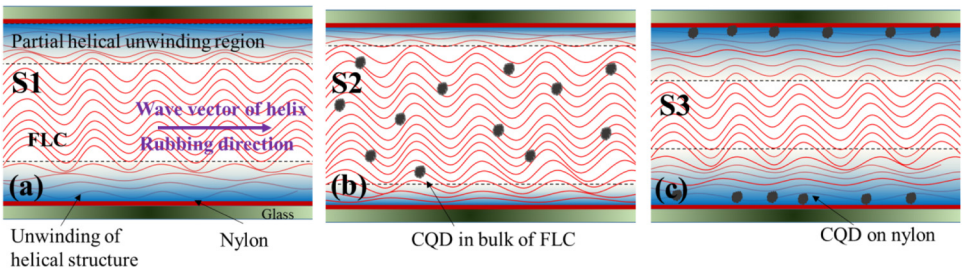

FIG. 7. Schematic of the helical structure at the interface of the strongly rubbed nylon coated glass substrate for (a) pure FLC, **S1**, (b) CQDs dispersed in the FLC, **S2**, and (c) CQDs deposited on the nylon 6/6 substrate, **S3**.

resulting in the significant change in the results, as discussed earlier. Figure 7(a) illustrates the usual helical formations and partial unwinding at the interface of the substrate. The partial unwinding varies largely from the substrate into the bulk of FLC of the **S1** sample. When the CQDs are dispersed into the bulk of FLC, **S2**, the FLC material attains the gain in the surface tension (94.35 mJ/m^2) as revealed by the contact angle [Fig. 6(b)] and the texture micrographs [Fig. 5(a)] and does not allow the helical structure to get unwound up to a large extent in comparison with the bare FLC. This is the reason for the nonobservation of *p*-UHM in these sample cells [Fig. 7(b)]. On the other hand, when the CQDs are deposited on the strongly rubbed surfaces, **S3**, the surface offers a greater anchoring energy (122.3 mJ/m^2) which supported the formation of localized domains [Fig. 5(c)]. This is the case of greater unwinding of a helical structure than the required one for the appearance of the *p*-UHM process and hence there is no appearance of the *p*-UHM in the **S3** sample cell also [Fig. 7(c)]. This infers that the partial helical unwinding is required up to a certain range below and above which the *p*-UHM process would not be appearing in the dielectric spectroscopy, as illustrated in the present study.

CONCLUSION

In conclusion, we have investigated the specificity of the interfacial interaction of the FLC material with a solid substrate via CQDs. The impact of CQDs on the partially unwound helical structure at the interface of FLC and solid substrate has been revealed. The surface anchoring mapping of the substrate has revealed that the surface anchoring and surface tension of the FLC material affect the *p*-UHM process. Thus, the surface anchoring plays a crucial role in the behaviour of FLC molecules in the medium thickness sample cells (~8–20 μm). The reduced surface anchoring energy (or the increased surface tension) of the FLC material by employing the CQDs with FLC has resulted in a modulation of the helical structure at the interface beyond the limitation of the favourable condition for the partial helical unwinding process.

The modification in the substrate surfaces of the sample cell by CQDs does not affect the basic parameters of the FLC materials other than the helicoidal structure at the interface. However, the parameters get changed if the CQDs are dispersed in the FLC material due to changes in surface tension. The optical textures have also shown that the CQDs deposited on the surface modify the helical structure mimicking the SSFLC state by generating the localized domains in the sample cell. This shows that the helicoidal structure at the interface of the FLC and the substrate surface is completely unwound due to the strong anchoring mediated by CQDs.

ACKNOWLEDGMENTS

We sincerely thank the Director, Dr. D. K. Aswal, National Physical Laboratory, New Delhi, for his continuous encouragement in the work. We would like to thank the Department of Science and Technology, New Delhi, India, for financial support through Project Grant No. GAP-150632 at NPL, New Delhi. We are thankful to Himanshu Mishra and Anchal Srivastava, Banaras Hindu University, Varanasi, India, for a fruitful discussion about the carbon quantum dots. L.K.G. and A.M.B. are thankful to the Council of Scientific and Industrial Research (CSIR) for the financial assistance under the NET-JRF fellowship and Emeritus Scheme, respectively.

REFERENCES

[1]N. A. Clark and S. T. Lagerwall, Appl. Phys. Lett. **36**, 899–901 (1980).
[2]S. Kaur, S. P. Singh, A. M. Biradar, A. Choudhary, and K. Sreenivas, Appl. Phys. Lett. **91**, 023120–023122 (2007).
[3]A. Chaudhary, S. Kaur, G. Singh, J. Prakash, A. K. Thakur, and A. M. Biradar, J. Appl. Phys. **101**, 074112–074116 (2007).
[4]S. Kaur, A. K. Thakur, S. S. Bawa, and A. M. Biradar, Appl. Phys. Lett. **88**, 122905–122907 (2006).
[5]H. Furue, T. Takahashi, and S. Kobayashi, Ferroelectrics **244**, 75–82 (2000).
[6]T. Uchida, M. Hirano, and H. Sakai, Liq. Cryst. **5**, 1127–1137 (1989).
[7]A. M. Biradar, D. Kilian, S. Wrobel, and W. Haase, Liq. Cryst. **27**, 225–231 (2000).
[8]P. M. Lagarde and G. Durand, J. Phys. France **42**, 269–275 (1981).
[9]Y. P. Panarin, Y. P. Kalmykov, S. T. Mac Lughadha, H. Xu, and J. K. Vij, Phys. Rev. E **50**, 4763–4772 (1994).
[10]R. B. Meyer, Mol. Cryst. Liq. Cryst. **40**, 33–48 (1977).
[11]A. D. Rey, Phys. Rev. E **53**, 4198–4201 (1996).
[12]A. Choudhary, A. Bawa, Rajesh, S. P. Singh, and A. M. Biradar, Phys. Rev. E **95**, 062702–062709 (2017).
[13]A. Bawa, L. K. Gangwar, A. Dhingra, A. Choudhary, Rajesh, S. P. Singh, and A. M. Biradar, Liq. Cryst. **46**(2), 166–175 (2019).
[14]L. K. Gangwar, A. Bawa, A. Choudhary, S. P. Singh, Rajesh, and A. M. Biradar, Phys. Rev. E **97**, 062707–062713 (2018).
[15]S. S. Bawa, A. M. Biradar, and S. Chandra, Jpn. J. Appl. Phys. **26**, 189–192 (1987).
[16]J. Goldstone, Nuovo Cim. **19**, 154–164 (1961).
[17]Y. Nambu, Phys. Rev. **117**, 648–663 (1960).
[18]R. Blinc and B. Zeks, Phys. Rev. A **18**, 740–745 (1978).
[19]B. K. Urbanc and B. Žekš, Phys. Rev. E **52**, 3892–3903 (1995).
[20]L. C. Huang and C. M. Fu, Acta Phys. Pol. A **129**, 97–102 (2016).
[21]A. V. Emelyanenko, E. P. Pozhidaev, N. M. Shtykov, and V. E. Molkin, J. Soc. Inf. Disp. **16**(8), 811 (2008).
[22]Q. Liang, W. Ma, Y. Shi, Z. Li, and X. Yang, Carbon **60**, 421–428 (2013).
[23]I. Dierking, G. Scalia, P. Morales, and D. LeClere, Adv. Mater. **16**, 865–869 (2004).
[24]H. Qi and T. Hegmann, J. Mater. Chem. **18**, 3288–3294 (2008).
[25]F. V. Podgornov, A. M. Suvorova, A. V. Lapanika, and W. Haase, Chem. Phys. Lett. **479**, 206–210 (2009).
[26]J. Prakash, A. Choudhary, D. S. Mehta, and A. M. Biradar, Phys. Rev. E **80**, 012701–01276 (2009).
[27]P. Arora, A. Mikulko, F. V. Podgornov, and W. Haase, Mol. Cryst. Liq. Cryst. **502**, 1–8 (2009).
[28]X. Y. Xu, R. Ray, Y. L. Gu, H. J. Ploehn, L. Gearheart, K. Raker, and W. A. Scrivens, J. Am. Chem. Soc. **126**, 12736–12737 (2004).
[29]H. P. Liu, T. Ye, and C. D. Mao, Angew. Chem. Int. Ed. **46**, 6473–6475 (2007).
[30]R. Liu, D. Wu, S. Liu, K. Koynov, W. Knoll, and Q. Li, Angew. Chem. Int. Ed. Engl. **48**(25), 4598–601 (2009).
[31]F. Wang, S. P. Pang, L. Wang, Q. Li, M. Kreiter, and C.-Y. Liu, Chem. Mater. **22**, 4528–4530 (2010).
[32]X. H. Wang, K. G. Qu, B. L. Xu, J. S. Ren, and X. G. Qu, J. Mater. Chem. **21**, 2445–2450 (2011).
[33]S. Y. Lim, W. Shen, and Z. Gao, Chem. Soc. Rev. **44**, 362–381 (2015).
[34]A. P. Demchenko and M. O. Dekaliuk, Methods Appl. Fluoresc. **1**, 042001 (2013).
[35]S. N. Baker and G. A. Baker, Angew. Chem. Int. Ed **49**, 6726–6744 (2010).
[36]S. T. Yang, L. Cao, P. G. Luo, F. S. Lu, X. Wang, H. F. Wang, M. J. Meziani, Y. F. Liu, G. Qi, and Y.-P. Sun, J. Am. Chem. Soc. **131**, 11308–11309 (2009).
[37]R. K. Shukla, K. K. Raina, V. Hamplová, M. Kašpar, and A. Bubnov, Phase Transit. **84**, 850–857 (2011).

[38]R. K. Shukla, J. Mirzaei, A. Sharma, D. Hofmann, T. Hegmann, and W. Haase, RSC Adv. **5**, 34491–34496 (2015).
[39]J. Mirzaei, M. Reznikov, and T. Hegmann, J. Mater. Chem. **22**, 22350–22365 (2012).
[40]M. Urbanski, J. Mirzaei, A. Sharma, D. Hofmann, H. S. Kitzerow, and T. Hegmann, Liq. Cryst. **43**, 183–194 (2016).
[41]L. A. Bresnev, L. M. Blinov, M. A. Osipov, and S. A. Pikin, *Ferroelectric Liquid Crystals* (Gordon and Breach Science Publishers, San Antonio, TX, 1988).
[42]N. K. Adam, Nature **180**, 809–810 (1957).
[43]N. B. Vargaftik, B. N. Volkov, and L. D. Voljak, J. Phys. Chem. Ref. Data **12**, 817–820 (1983).